RESEARCH ARTICLE

Selection of corn harvester navigation route based on improved ant colony algorithm

Zhengguo Lu[1], Lili Yu[2, *]

[1]Institute for Ethnic Groups Attached, Hebei Normal University, Shijiazhuang, Hebei, China. [2]Software Engineering Department, Shijiazhuang Information Engineering Vocational College, Shijiazhuang, Hebei, China.

Received: June 12, 2024; **accepted:** August 30, 2024.

Agricultural mechanization is a core part of the development of modern agriculture and involves the use of various mechanized tools and systems to automate traditional agricultural processes, thereby improving production efficiency, reducing labor costs, and increasing crop yields. Mechanized operations include land consolidation, sowing, fertilization, plant protection, harvesting, and other links. Among them, harvesting is a particularly critical link because it is directly related to the rate of crop loss and harvest quality. With the progress of technology, automated and intelligent harvesting robots have become an important development direction of agricultural mechanization. The route selection method of corn harvester based on the improved ant colony algorithm was proposed in this study to achieve the accurate route selection and planning of corn harvester and the improvement of the quality and efficiency of corn harvest. By applying the mobile robot dynamic path planning method based on the improved ant colony algorithm, target point adaptive heuristic function was used to improve the convergence speed of the algorithm. Particle swarm optimization was used to optimize the important parameters of the improved ant colony algorithm, and the dynamic path planning of mobile robot based on improved ant colony algorithm was realized. The color characteristics of visual navigation image were analyzed to remove the shadow interference, and the method of cumulative hop G component was used to determine the candidate point. In the area of interest, the candidate point was searched in the G component vertical accumulative value after removing shadow interference. The variance of the candidate points with good convergence in the semi-part of the image was calculated to determine the known point. The Hough transform of the known point was used to fit the navigation line of the boundary of the corn column. The continuous mutation of the R component was judged for whether the harvester reached the end of the field to realize the accurate selection of the navigation route of the corn harvester. The proposed method could accurately detect the image of the boundary line of corn. The harvested land was detected on the left side while the right harvest was not harvested with the accuracy of 99.2%. The average processing time per frame was 50.13 ms. The field end image could also be detected accurately. The shadow of the corn column did not affect the detection of the navigation line. The proposed method had a certain anti-interference to the overlapping of the middle and low level rice leaves. The proposed method could effectively segment the ratooning rice plants and path. The navigation path in the low layer under the complex background was extracted for the ratooning rice plant, which could effectively remove the corn column shadow interference and quickly detect the navigation line of the corn harvest and the field end. It has high anti- interference and operational efficiency on the overlapping of middle and low layer rice leaves.

Keywords: improved ant colony algorithm; corn harvester; navigation route; selection; robot; pheromone.

[*]**Corresponding author:** Lili Yu, Software Engineering Department, Shijiazhuang Information Engineering Vocational College, Shijiazhuang 052161, Hebei, China. Email: yll0220_2024@163.com.

Introduction

With the continuous increase of the global population and the growing demand for agricultural production, the development of modern agriculture is faced with multiple challenges such as low production efficiency, high labor cost, and insufficient resource utilization efficiency [1]. In this context, agricultural mechanization is widely regarded as a key means to improve the efficiency and quality of agricultural production. Mechanized operations cover several links, of which the harvest link is particularly important because the harvest efficiency directly affects the rate of crop loss and the final product quality [2]. Therefore, to improve the level of automation of agricultural machinery, especially the intelligence and automation of harvesting machinery, has become the focus of the current development of agricultural science and technology. At present, although some progress has been made in agricultural mechanization domestically and internationally, there are still many challenges in path planning.

Many scholars have certain research on path planning. Li *et al*. proposed an angle-guided ant colony algorithm (ACA) to solve the problem that ACA was prone to local optimization and slowed convergence in mobile robot path planning. In the node selection, angle factor was integrated into the heuristic information of ACA to guide the search direction of ants and improve the search efficiency. In addition, the algorithm also updated the pheromone differentially for paths with different qualities and introduced the pheromone chaotic disturbance update mechanism. According to the simulation results, the algorithm performed well in global search ability, could jump out of the local optimal solution, and could quickly converge to the global optimal solution [3]. Tian introduced an optimal path planning method based on the improved ACA, which aimed to overcome the problems of poor convergence and obstacle avoidance in the planning of the optimal path of robots by traditional methods. Firstly, the environment information and robot motion state information were obtained, and then the pheromone was updated according to the adaptive transformation heuristic function of the target point and the wolf pack allocation principle. According to the experimental results, the overall mean value of collision avoidance of this method was 0.97, indicating that the planning performance was significantly better than that of similar planning methods and had considerable application value [4]. Rath *et al*. used a combination of genetic algorithm and neural network to control the navigation of humanoid robots in a given complex environment. A genetic algorithm controller was used to generate the initial turning angle of the robot, and then the genetic algorithm controller was mixed with a neural network controller to generate the final turning angle. From the simulation and experimental results, satisfactory consistency was observed in terms of navigation parameters with minimal error limitation, which proved the correct operation of the proposed hybrid controller [5]. Garcia *et al*. generated efficient collusion-free multi-robot path planning solutions for human-controlled environments and extended previous research. This scheme combined the optimization capability of A* algorithm and the search capability of coevolutionary algorithm. The result was a set of collision-free routes that could be derived from the A* algorithm in the process of coevolution. This set of routes was generated in real time and could be implemented on edge computing devices [6]. However, there are still some limitations. For example, most of the methods cannot effectively identify the distance between crop rows and rows in complex agricultural environments, resulting in inefficient harvesting and unnecessary crop losses. In the face of complex background and shadow interference, it showed obvious shortcomings.

To solve the problems of low efficiency and crop loss of corn harvester in the process of harvesting, and the existing path planning methods are difficult to adapt to the dynamic changes of agricultural environment, a dynamic

path planning method of corn harvester based on improved ACA was proposed in this research. The improved ACA was used to realize fast and effective path planning in dynamic environment, and the convergence speed of the algorithm was enhanced by the adaptive heuristic function of the target point. Visual image processing technology was introduced to analyze image color features and eliminate shadow interference to accurately evaluate candidate points and determine navigation routes. This study combined the improved ACA with visual navigation technology and put forward an efficient dynamic path planning solution. The particle swarm optimization (PSO) algorithm was used to optimize the key parameters of the improved ACA, which made the whole algorithm more efficient. This study would provide an important reference for the research and application of intelligent agricultural machinery and equipment, and also promote the autonomous operation ability of agricultural machinery under more complex and changeable environmental conditions, laying the foundation for the sustainable development of agriculture in the future.

Materials and methods

Image acquisition, analysis, and preprocessing

A general digital camera was fixed to the rearview mirror on the side of the corn harvester in front of the boundary line with the height about 2 m and the down-looking angle about 30°. The average speed of the harvester was 10 km/h. The scene color video images were captured in the process of harvesting with the frame rate of the video acquisition of 25 frames/s and the size of each frame of 640 × 480 pixels. During the harvest of the first season rice, the drainage roast field was used to help the harvester walk. For the complexity of the growth of leaf and rice pile in the ratooning rice, the appropriate color space was selected for image segmentation. The whole grayscale space was divided into regions and path regions of the ratooning rice plants with distinct gray values. The saturation (S) difference was used to segment the path from the complex image information.

Threshold Segmentation

The improved Otsu method was applied to obtain the initial threshold (T) of the S component and binary processing. When binarization, combining the histogram feature of S component, reducing the segmentation threshold properly could help to retain the characteristics of the plant and reduce the interference of the stem and leaf with different maturity. Therefore, the correction factor (a) was added to the segmentation threshold. The binarization of the S component was then with the threshold T-a. After multiple image tests, a was set to 12 to reach a satisfactory result. The farmland image was divided into the white plant area and the black path area, and the left and right boundary of the plants reflected the trend characteristics of the ratooning rice.

De-noising and other postprocessing

After the binary image was obtained, black holes appeared in the plant area and the white spot noises appeared in the path area, which introduced the noises for the young green weeds grown in the soil after the drainage of the field. The connectivity analysis of expansion region was first carried out for the 7 × 7 structural elements. The denoising method was used for the connected area. The area TH1 took 800 pixels to obtain a better result. Then, the 5 × 5 elements were used to carry out morphological closure to further remove the noise.

Dynamic path planning for mobile robot based on improved ant colony algorithm

To facilitate the search of the optimal path by ACA, the grid method was used to divide the environment, which assumed that the working space of the robot was a finite area on the two-dimensional plane, and the starting point and the target point were S and T, respectively. The optimization criterion of the path planning was for the shortest path, that was, to find the shortest path to avoid obstacles from S to T [7]. The grids were numbered in order from left to

right and from top to bottom. The robot could reach the adjacent grid in 8 directions including upper, down, right, left, upper right, upper left, lower right, and lower left. The workspace of the robot was made up of grids with M row and N column. The number of the row and column of the environmental grid corresponding to a random grid (R) was x and y with the relational expressions below.

$$x = \lfloor R / N \rfloor + 1 \tag{1}$$

$$y = R\%N + 1 \tag{2}$$

The map of the obstacle was represented by a two-dimensional array matrix map (M, N), which was given as follows.

$$map(p,q) = \begin{cases} 1, & There\ is\ obstacle\ on\ the\ grid\ (p,\ q) \\ 0, & Others \end{cases} \tag{3}$$

For the shortcomings of ACA such as slow search speed and easy to fall into local optimum, the pheromone update based on adaptive adjusting heuristic function and principle of wolf pack allocation was proposed [8].

Adaptive adjusting heuristic function

The probability of the transfer of ant a from the grid i to the j at the time t was defined as $p_{ij}^{a}(t)$ below.

$$p_{ij}^{a}(t) = \begin{cases} \dfrac{\tau_{ij}^{\alpha}(t)\eta_{ij}^{\beta}(t)}{\sum_{s \in allowed_a} \tau_{is}^{\alpha}(t)\eta_{is}^{\beta}(t)}, & if j \in allowd_a \\ 0, & otherwise \end{cases} \tag{4}$$

where $\eta_{ij}(t)$ was the heuristic function of the subsequent grid. $\tau_{ij}(t)$ was the concentration of pheromones remaining on the path <i, j> at the time t. α and β were the influence weights of the $\tau_{ij}(t)$ and $\eta_{ij}(t)$ on the whole transfer probability. $allowed_a$ was the grid number for the ant a allowed to select in the next step. In the traditional ant colony, the heuristic function of the subsequent grid $\eta_{ij}(t)$ was as follows.

$$\eta_{ij}(t) = \frac{1}{d_{ij}} \tag{5}$$

where d_{ij} was the distance from the grid of i to j. In the traditional ant colony, the heuristic weight difference between adjacent grid was not obvious, so the search efficiency of the algorithm was low. As the position of the target point was known, the distance $dis(h)(1 \le h \le 8)$ between the 8 grids and target point could be calculated. The heuristic weights of the surrounding grid were then adjusted adaptively in a certain proportion by the value of $dis(h)$. The smaller the value of $dis(h)$, the greater the heuristic weight of the h[th] grid. In this study, it was set to 1:2:3:3:4:4:5. If the target point of the mobile robot was on the lower right of the current point, the heuristic function of the grid around the current point would be:

$$\eta_{ij}(t) = \begin{cases} \varepsilon, \mathrm{j} = \mathrm{i} - \mathrm{N} - 1 \\ 2\varepsilon,\ j = i - N \quad or \quad j = i - 1 \\ 3\varepsilon,\ j = i - N + 1 \quad or \quad j = i + N - 1 \\ 4\varepsilon,\ j = i + 1 \quad or \quad j = i + N \\ 5\varepsilon,\ j = i + N + 1 \end{cases} \tag{6}$$

Pheromone updating mechanism based on the principle of wolf pack allocation

After n time, the ant colony completed a cycle of movement, leaving the pheromone on the path it passed, and the pheromone concentration would be distributed over time. The pheromone concentration on path <i, j> at the time t was defined as $\tau_{ij}(t)$, then the concentration at the time t + 1 was given as follows.

$$\tau_{ij}(t+1) = (1-\rho)\tau_{ij}(t) + \Delta\tau \tag{7}$$

$$\Delta\tau = \sum_{a}^{m} \Delta\tau_{ij}^{a} \tag{8}$$

where ρ was the pheromone volatilization coefficient. $\Delta\tau_{ij}^{a}$ was the pheromone concentration of the a[th] ant on the path <i, j> in this cycle. The ant-cycle computing model based on global information was used to obtain $\Delta\tau_{ij}^{a}$.

$$\Delta\tau_{ij}^{a}=\begin{cases}Q/L_a, if\ the\ ath\ ant\ pass\ through\ i,j\\0\quad\quad,Others\end{cases} \tag{9}$$

where Q was the constant of the pheromone concentration. L_a was the path length of ant a in this cycle. The pheromone was updated by using the principle of wolf pack allocation. The path pheromone concentration according to the principle of wolf pack allocation was updated by the equations below.

$$\tau_{ij}(t+1)=(1-\rho)\tau_{ij}(t)+\sum_{a=1}^{m}\Delta\tau_{ij}^{a}\Delta^{*}\tau_{ij}-\Delta^{**}\tau_{ij} \tag{10}$$

$$\Delta^{*}\tau_{ij}=\begin{cases}\delta(Q/L^{*}), Local\ optimal\ path\ passing\ through\ i,j\\0,\quad\quad,Others\end{cases} \tag{11}$$

$$\Delta^{**}\tau_{ij}=\begin{cases}\omega(Q/L^{**}), Local\ worst\ path\ passing\ through\ i,j\\0,\quad\quad,Others\end{cases} \tag{12}$$

where L^{*} and L^{**} were the lengths of local optimal path and local worst path. δ and ω were the numbers of local optimal ants and local worst ants.

Parameter optimization based on particle swarm optimization

The important parameters of the improved ACA were the influence weights of pheromone concentration and heuristic function on the transfer probability α and β, pheromone volatilization coefficient ρ, pheromone concentration constant Q, and heuristic function ε. Parameters were selected by experience and optimized using PSO, a novel evolutionary algorithm, that assumed D-dimensional search space and m particle number. For a particle 1, the position and velocity were x_1 and v_1, respectively.

$$x_1=(x_{l1},...,x_{ld},...,x_{lD}) \tag{13}$$

$$v_1=(v_{l1},...,v_{kl},...,v_{lD}) \tag{14}$$

where $1\le l\le m, 1\le d\le D$. The best position of the solution space of the particle 1 was $P_l=(P_{l1},P_{l2}...,P_{lD})$. The position of the particle with the optimal fitness was $P_g=(P_{g1},P_{g2}...,P_{gD})$. The evolution equation of particle swarm was then given as

$$V_{kl}^{k+1}=wV_{kl}^{k}+c_1r_1(P_{kl}^{k}-X_{kl}^{k})+c_2r_2(P_{gd}^{k}-X_{kl}^{k}) \tag{15}$$

$$X_{kl}^{k+1}=X_{kl}^{k}+V_{kl}^{k+1} \tag{16}$$

where w was inertia weight. c_1 and c_2 were learning factors. r_1 and r_2 were random numbers with uniform distribution in $[0,1]$. k was the number of iterations. The range of changes of the position and velocity of the d[th] particle were $[XMIN_d, XMAX_d]$ and $[VMIN_d, VMAX_d]$. If the value calculated by equations 15 and 16 exceeded this range, it was set as the boundary value.

Navigation route detection method for corn harvester based on image processing

Detection Navigation Path Point Set

The total number of black spots in each row of the image was detected based on the characteristics of the left and right boundary region of the plant. The steps of the extraction of the set point were (1) building an empty matrix A, denoted as M*N. Initializing temporary variables m = 0 and k = 0; (2) scanning the image after denoising line by line. Assuming the first point of the scanned image was the upper left corner of the image. If the pixel value of the current image point (i, j) was 0, $m{+}{+}$ and $k=m/2$; (3) scanning the column in the step (2) again to determine the point coordinates in the path. If the pixel value of the current image point (i, j) was 0, $k=--$. Until k==0, the coordinates (i, j) were recorded. The pixel value 255 was stored in A; (4) stop scanning until M row, otherwise

continue the step (2). The A was stored in the denoised image. The extraction result showed the mean position of the point in the path. Because the image size was larger and in the presence of noise, the detection results of local point had deviation, but did not affect the overall results [9, 10]. Therefore, the algorithm had certain anti-interference to the cavitation and spot noise in the binary image.

Extraction of navigation line

The information of the navigation line could be extracted after the path fitting point was detected. For the crops, the linear path model was used. The navigation line could be detected according to the binary image of the ratooning rice plant, so that the wheeled harvester walked along the navigation line to reduce the pile compression rate. The Hough transform has good adaptability to the random noise of the image and the missing part of the information [11]. Standard Hough transform and Hough transform based on known points were compared in this study. Opencv provided a standard Hough transform function - Houghlines to detect a straight line, while Hough transform based on the known point was used to extract the information of the navigation line. Because the growth of rice leaves at the end of the image was relatively irregular, the selection of known points started from the image M/2 row to scan all the path fitting points of the image and calculate the average position of its abscissa and ordinate, which was regarded as known points.

Image detection of boundary line of corn column

During navigation, a series of natural factors such as crops, weeds, and soil interweave in the process of navigation formed a complex detection environment. Meanwhile, camera resolution, color difference, and the vibration of cameras also affected the detection results [12]. This study first assumed the boundary of corn column as a straight line, and then analyzed the color features of the color image of red (R), green (G), and blue (B) to obtain the candidate points. A specific point as the known points was obtained by variance within a specific area of candidate points. Hough transform of the known point was then used to obtain the navigation line.

First frame image detection

Assumed that the upper left corner of the set image was the origin of the coordinates, and the right direction was the x positive direction and down to the y positive direction, x size was the x direction width and y size was the y direction height. The following steps were processed to obtain the first frame image.

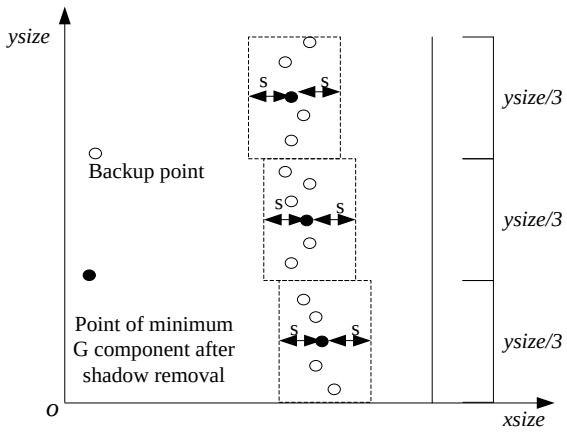

Figure 1. Backup points of first frame (Note: interesting region located in the dotted line boxes: x size was width of the image. Y size was the height of the image. s was the number of pixel).

(1) On the whole x direction [0, x size - 1], the entire image was divided into 3 regions along the y direction (Figure 1). The array Pt [y size] was defined to store the candidate point, and the initial value was set to −1. The range of the y direction was defined as $[sy_n,\ ey_n]$.

$$[sy_n, ey_n] = [(n-1)\text{gysize}/3, nysize/3] \quad (17)$$

where, sy_n and ey_n were the starting and ending positions of the n^{th} region. n was an integer variable with the range of $[1,3]$.

(2) The input color image was scanned line by line. The arrays $buff\_r[xsize]$, $buff\_\text{g}[xsize]$,

and $buff\_b[xsize]$ were used to store the vertical cumulative pixel values of R, G, and B components in the processing window. The mean of the $buff\_r$ and $buff\_b$ was obtained as $mean\_r$ and $mean\_b$. If $mean\_r >= mean\_b$, color = 1, otherwise, color = 2.

(3) If the cumulative value $buff\_b[i] - buff\_g[i] < 0 \ (0 \le i \le xsize - 1)$, the corn plants had a shadow. Then set $buff_g[i] = 255$gsize_y(size_y = ey − sy + 1), otherwise, keep $buff\_g[i]$ unchanged. The smoothing processing of the array $buff\_g$ was carried out with the step length of 6, and the element with the smallest pixel value was obtained. Then the cross coordinates of this point were recorded as pos.

(4) Taking pos as the center, s pixels were extended to the left and right (set $s = xsize/40$). The width of the 3 dynamic region of interest was set in the range of the x direction as follows.

$$[sx_n, ex_n] = [(pos - s), (pos + s] \quad (18)$$

where pos was the pixel minimum abscissa. To remove the shadow interference, if color = 1, the R component was used as the processing object XX. If color = 0, the B component was used as the processing object XX. Each pixel in the processing range was scanned in turn. If the value of the XX component was less than or equal to the value of the G component, G was set to $(g\max - g\min)/2$, otherwise, save the original value of G.

(5) The known point was found in the 1/2 of the upper part of the image. The variance and mean of the value of $Pt[ysize/2] \sim Pt[3$gysize$/4 - 1]$ whose value was not -1 were denoted as sd1 and mean1. The variance and mean of the value of $Pt[3$gysize$/4] \sim Pt[ysize - 1]$ whose value was not -1 were denoted as sd2 and mean2. If sd1>sd2, $(mean2, 3$gysize$/8)$ was taken as the known point. If sd1<=sd2, $(mean1, ysize/8)$ was taken as the known point.

(6) Hough transformation of known points was used to fit the navigation line, and the horizontal coordinates of the data were recorded in the array $Hp[ysize]$.

The steps (2) ~ (4) were repeated to obtain all the candidate points in the first frame of the 3 dynamic regions of interest (Figure 1).

Non-first frame image detection

The region of interest of the non-first frame image was determined by the angle of the Hough line angle and image midperpendicular with the following steps [13].

(1) Setting $sy = 0$ and $ey = ysize - 1$, the coordinates of the first point $(Hp[0], 0)$ and the last point $(Hp[ysize - 1], ysize - 1)$ on the Hough line were taken as parameters. The angle θ of the Hough line of the previous frame and midperpendicular were calculated as below.

$$\theta = \arctan((ysize - 1)/(Hp[ysize - 1] - Hp[0])) \quad (19)$$

The processing range (dis) was given as

$$dis = \partial$gθ$/3 + \beta \quad (20)$$

where ∂ was the inter pixel distance. β was the cardinal number. In this study, $dis \le xsize/20$.

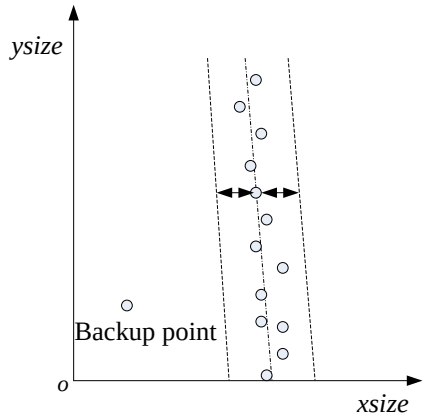

Figure 2. Backup points of non-first frame. dis was the number of pixels.

(2) The candidate point was detected. $(Hp[j+H/2], j)$ was taken as the midpoint. Extend the dis pixels to the left and right as the processing range (sx, ex). If the left side had been harvested, it could find the location of the largest trough point in the ascending direction of the peak value and trough difference. If the right side had been harvested, it could find the location of the largest trough point in the descending direction of the smoothing value [14]. The x coordinates of the wave valley point were recorded as minpos (Figure 2).

(3) To remove the point with a larger error, setting the threshold T as T = dis. The minpos and the same position point were compared. If $|\min pos - Hp[j+H/2]| \le T$, $Pt[j+H/2] = \min pos$. If $|\min pos - Hp[j+H/2] > T|$, $Pt[j+H/2] = Hp[j+H/2]$.

(4) Letting $j = j + \mathrm{H}$, the steps (2) and (3) were repeated. When $j < ysize - 1 - H$, stop the cycle.

(5) The same method of the first frame was used to calculate the known point.

(6) The navigation curve was fitted and the array of points on the navigation line were recorded in Hp.

(7) Whether the algorithm reached the end of the field was then judged.

Image detection algorithm for the field end

For the non-first frame image, the field end detection method was as follows.

(1) In the harvested area near Hough line of the last frame, the rectangle with the upper left coordinates $(Hp[ysize/n1]-50, ysize/n1)$ and lower right coordinates $(Hp[ysize/n2], \mathrm{ysize}/\mathrm{n}\,2)$ was taken as the processing region (n1 = 16 and n2 = 6).

(2) In the processing region, the R component accumulated horizontally [15]. Accumulative values were recorded in the array $M[50]$.

(3) The variance sd of the array M was calculated.

(4) If sd was greater than the threshold T1 (T1 = mean/20e), return to TRUE, otherwise return to FALSE. If sd was more than 10 times greater than the threshold, it was judged to have reached the field end.

Results

Image detection of boundary line of corn column

In determination of the known point and the processing region, the cumulative method of G component cumulative hop was used to make the detection more accurate and reasonable [16]. Figure 3 illustrated the real time collected images with/without the interference of the shadow of the corn column (Figures 3a and 3b). The wave valley point with the maximum difference was the candidate point (Figures 3c and 3d). The accuracy of finding the candidate point was improved after removing the shadow interference, which was verified by Figures 3a and 3b that the left side was harvested, and the right was not. The Hough transformation of known point was a good way to fit the navigation line [17]. The results of the navigation line detection corresponding to that in Figures 3a and 3b were shown in Figures 4a and 4b. The actual working environment of the video was tested. The statistical test results showed that, in the total of 3,777 frames of the video sample, error detection was in 30 frames. Among them, the candidate points biased due to the dry corn harvest area in 27 frames, and the other 3 frames was in the corn row. Because the limit of the detection range was set, the detection error did not affect the correct detection of subsequent frames [18]. The detection accuracy was 99.2%, and the average processing time of each frame was 50.13 ms.

Field end image detection

The original image and the test results of navigation end line were shown in Figure 5 as the solid line. When the environment was complex,

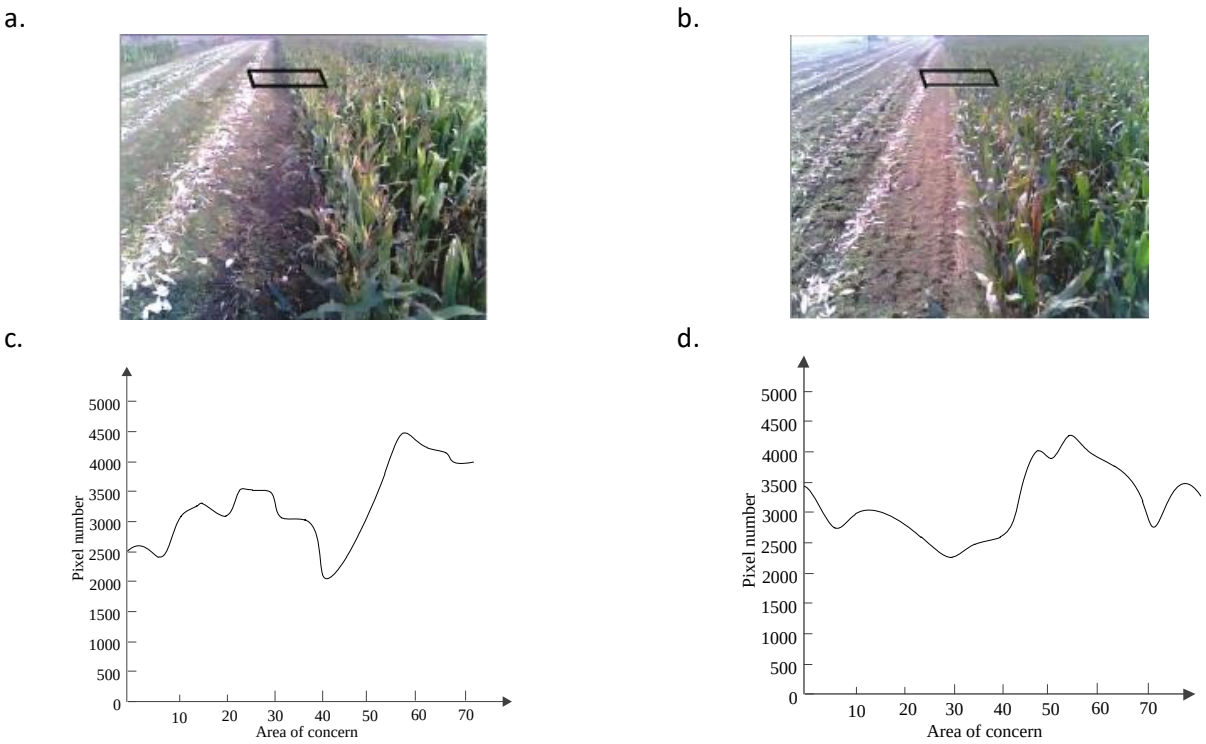

Figure 3. Detection line and vertically integrated graph of G components. **a.** image with the interference of the shadow of the corn column. **b.** image without interference of the shadow of the corn column. Black box was the G component vertical cumulative region in the region of interest from the j + H line to the j line when j = 100. **c.** vertically integrated graph of G components in image a. **d.** vertically integrated graph of G components in image b.

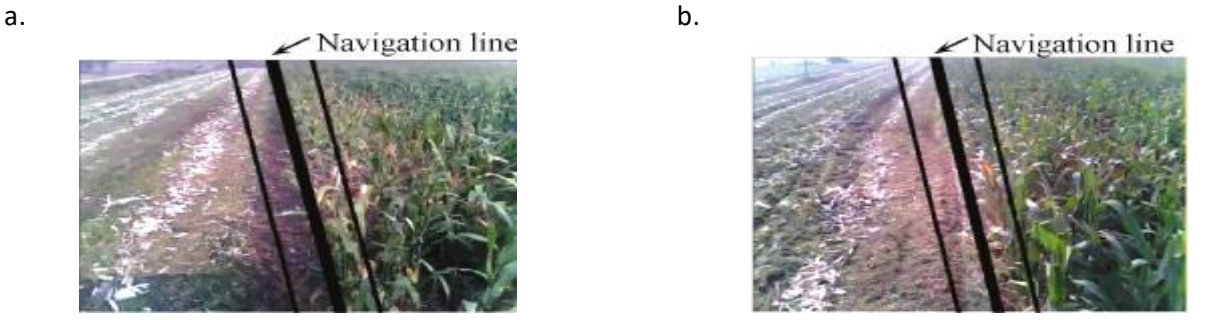

Figure 4. Detection result of navigation line with different light conditions. **a.** detection navigation line of Figure 3a image. **b.** detection navigation line of Figure 3b image.

Figure 5. Detection of the field was end.

the multiple mutation of the color component was used to judge the field end, which could effectively avoid the misjudgment. The mutation of the R component was considered to judge the field end. To verify the validity of this method, a comparison was carried out to collect the images of the ratooning rice at different shooting angles in the experimental field. The image was with 419

× 310 pixels. Five ratooning rice images were compared with standard Hough and Hough based on known point. To verify the correctness and feasibility of the proposed method, a simulation experiment was carried out. The robot working environment was divided into a 20×20 grid, and the width and width of each grid were 20 units. In ACA, the number of populations was 30 and the maximum number of iterations was 100. In this study, PSO was applied to optimize the important parameters of the improved ACA. The number of particles was 20, the maximum iteration number was 30, the inertia weight w was 0.729, and the learning factors c_1 and c_2 were 1.4962. The range of changes of important parameters in the improved ACA was shown in Table 1.

Table 1. The change range of important parameters in improved ant colony algorithm.

Range	∂	β	ρ	Q	ε
Minimum value	0	0	0	100	0
Maximum value	10	20	1	1,000	20

When the number of the starting and the target grid were 21 and 378, respectively, the optimal combination of the important parameters of the ACA was found by the PSO algorithm as $\partial=1,\beta=7,\rho=0.367,Q=333,\varepsilon=2$. The dynamic path planning simulation process of mobile robot based on improved ACA showed that the block was a static obstacle, and the dynamic obstacle was a square with a radius of 5 units (Figure 6).

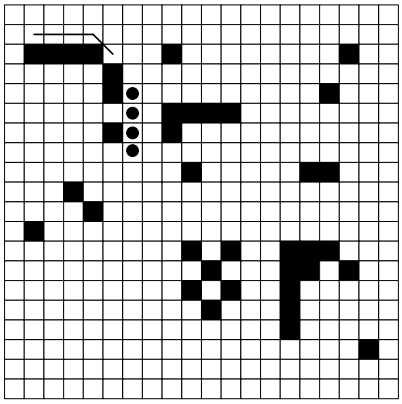

Figure 6. The robot collided with a dynamic obstacle.

The improved ACA could find the global optimal path. The grid numbers of the mobile robot passing through were 21, 22, 23, 24, 45, 46, 67, 87, 107, 127, 148, 168, 189, 210, 231, 252, 273, 293, 313, 354, 375, 376, 377, 378. It was supposed that the velocity of robot walking was 20 units/sec, and the time of turning around each corner was 1 s.

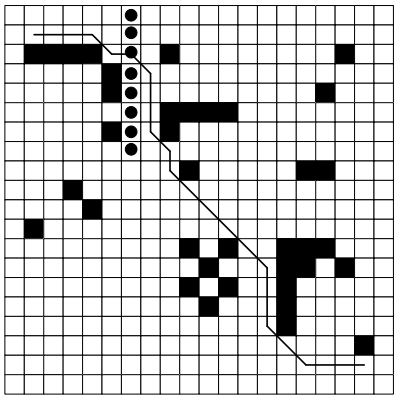

Figure 7. The final path of improving the planning of ant colony algorithm.

The traditional ACA, improved ACA, and A* algorithm was compared, and the optimal performance of the three algorithms was shown in Table 2. The improved ACA could avoid the search in local optimum and reduce the walking time of the robot. The simulation results proved that the improved ACA could effectively solve the robot's dynamic path planning problem.

Table 2. Performance comparison of three algorithms.

Algorithm	Path length (Pixel)	Time consuming (s)
A* algorithm	602.842	40.1421
Ant colony algorithm	579.412	38.9706
Improved ant colony algorithm	562.8427	38.1421

Discussion

The shadow of corn column causes great disturbance to the accuracy of navigation line

Table 3. Comparison of time between standard Hough and known point based on Hough.

Image No.	1	2	3	4	5
Time consuming of standard Hough method (s)	0.081	0.089	0.083	0.092	0.097
Time consuming of Hough based on the known point (s)	0.065	0.062	0.061	0.064	0.067

detection. In this study, the influence of the shadow was removed by comparison of G component and other color components. The R or B component was identified by the color identification method, and then compared with the G component. The G component which was greater than R component or B component was set as a fixed value, while retained the G component with smaller value, which could effectively remove the corn column shadow interference [19]. The results of the navigation line detection showed that the presence of the shadow of the corn column did not affect the detection results of the navigation line. The fitting line was in good agreement with the actual observed target line (corn harvest boundary line). Although there was corn shadow interference, because the G component was strengthened and the shadow interference was eliminated, the navigation line detection result was not affected by the corn column shadow. The extracted Hough line based on the known point kept the precision of the standard Hough. The time-consuming comparison of the 2 algorithms showed that the Hough based on known points took less time and was easy to meet the real-time requirement of the auxiliary driving (Table 3). The proposed method had good adaptability to navigation path detection under the condition of rice leaf overlapping. The fitted navigation line basically reflected the trend characteristics of ratooning rice and was consistent with human vision sense judgment [20]. The navigation path fitted by Hough transform based on known points was to improve the efficiency of navigation line detection [21]. The experimental results demonstrated that the proposed method had some anti-interference to the overlapping of middle and low layer rice leaves. This study proposed dynamic path planning for the mobile robot based on improved ACA. The dynamic area of interest was set for the detection of navigation line using different methods of first and non-first frame images, reducing the amount of data processing while adapting to the tilting of target line and ridge line. Multiple mutation of color component R was used to judge the field end in the case of the complex field end image for the detection of the termination line of the field end navigation [22]. The known points were found in the semi-part of the image in the process of real time navigation. The results confirmed that the judgment of the navigation line was accurate, and the judgment of the field ends coincided with the reality. An improved ACA was used to make dynamic path planning for the mobile robot with the improved speed of search. Based on principle of wolf pack allocation, the ants with local optimal paths in each cycle were found. The released pheromone quantity was increased, and pheromones released by ants on local worst path were removed. The interference of the pheromone on the worst path was avoided, and the convergence speed was improved. The improved ACA was used to realize the dynamic path planning of the mobile robot, and the feasibility and effectiveness of the path planning method were proved.

Acknowledgements

The research was supported by Shanxi Province Educational Science Planning Project (Grant No. GH-220794 and GH-220970), Scientific Research Fund Project from Shanxi Vocational University of Engineering Science and Technology (Grant No. KJ-202204).

References

1. Wagner D, Jones JB, Gordon DM. 2004. Development of harvester ant colonies alters soil chemistry. Soil Biol Biochem. 36(5):797-804.
2. Gordon DM. 2013. The rewards of restraint in the collective regulation of foraging by harvester ant colonies. Nature. 498(7452):91-93.
3. Li Y, Huang Y, Ge L, Li X. 2022. Mobile robot path planning based on angle-guided ant colony algorithm. Int J Swarm Intel Res. 13(1):177-195.
4. Tian H. 2021. Research on robot optimal path planning method based on improved ant colony algorithm. Int J Comput Sci Math. 13(1):80-92.
5. Rath AK, Parhi DR, Das HC, Kumar PB, Mahto MK. 2021. Design of a hybrid controller using genetic algorithm and neural network for path planning of a humanoid robot. Int J Intel Unmanned Syst. 9(3):169-177.
6. Garcia E, Villar JR, Tan Q, Sedano J, Chira C. 2023. An efficient multi-robot path planning solution using A* and coevolutionary algorithms. Integr Comput-Aided Eng. 30(1):41-52.
7. Ingram KK, Gordon DM. 2013. Colony life history and lifetime reproductive success of red harvester ant colonies. J Anim Ecol. 82(3):540-550.
8. Pinter-Wollman N, Gordon DM, Holmes S. 2012. Nest site and weather affect the personality of harvester ant colonies. Behav Ecol. 23(5):1022-1029.
9. Schafer RJ, Holmes S, Gordon DM. 2006. Forager activation and food availability in harvester ants. Anim Behav. 71(4):815-822.
10. Schwander T, Cahan SH, Keller L. 2006. Genetic caste determination in pogonomyrmex harvester ants imposes costs during colony founding. J Evol Biol. 19(2):402-409.
11. Zee J, Holway D. 2006. Nest raiding by the invasive argentine ant on colonies of the harvester ant, pogonomyrmex subnitidus. Insectes Sociaux. 53(2):161-167.
12. Xu Y, Lin ZX, Yao JM. 2016. Target search path fuzzy control of robot navigation. Comput Simul. 33(10):300-304.
13. Jiang J, Zhang HC. 2016. Research on robot path planning based on improved potential field ant colony algorithm. Comput Simul. 33(9):329-334.
14. Cai Z, Chen T, Zeng C. 2016. A global approach to the optimal trajectory based on an improved ant colony algorithm for cold spray. J Therm Spray Technol. 25(8):1-7.
15. Brosset D, Claramunt C. 2011. An experimental ant colony approach for the geolocation of verbal route descriptions. Knowl-Based Syst. 24(4):484-491.
16. Fei T, Zhang LY, Zhang J. 2016. Research of emergency logistics distribution routing optimization based on simulated annealing ant colony optimization. IEEE Trans Softw Eng. 42(2):170-186.
17. Li XY, Tian P, Leung SCH. 2009. An ant colony optimization metaheuristic hybridized with tabu search for open vehicle routing problems. J Oper Res Soc. 60(7):1012-1025.
18. Wang J, Zhang L, Lu F. 2014. The segmentation of wear particles in ferrograph images based on an improved ant colony algorithm. Wear. 311(1-2):123-129.
19. Enzmann BL, Nonacs P. 2010. Digging beneath the surface: Incipient nest characteristics across three species of harvester ant that differ in colony founding strategy. Insectes Sociaux. 57(1):115-123.
20. Gordon DM, Guetz A, Greene MJ. 2011. Colony variation in the collective regulation of foraging by harvester ants. Behav Ecol. 22(2):429-435.
21. Enzmann BL, Gibbs AG, Nonacs P. 2014. The cost of being queen: investment across pogonomyrmex, harvester ant gynes that differ in degree of claustrality. J Insect Physiol. 70(11):134-142.
22. Udiani O, Pinter-Wollman N, Yun K. 2015. Identifying robustness in the regulation of collective foraging of ant colonies using an interaction-based model with backward bifurcation. J Theor Biol. 367(9):61-75.